size was found to be ~120 nm in sample A and ~40 nm in sample B. The particles of sample A (α-quartz) had a sheet-like morphology, while the particles of sample B showed two distinct morphologies (sheet and rods). In addition to silica, the soils were also rich in oxides of iron, magnesium and aluminium. Essential plant nutrients like potassium and calcium were also present in them. This study shows that termite soils need to be analysed before being used for any specific application, as composition and morphology may vary from location to location.

1. Semhi, K., Chaudhuri, S., Clauer, N. and Boeglin, J. L., Impact of termite activity on soil environment: a perspective from their soluble chemical components. *Int. J. Environ. Sci. Technol*., 2008, **5**, 431–444.
2. Jouquet, P., Mamou, L., Lepage, M. and Velde, B., Effect of termite on clay minerals in tropical soils: fungus-growing termites as weathering agents. *Eur. J. Soil Sci*., 2002, **53**, 521–527.
3. Lobry, L. A., Bruyn, De and Conacheri, A. J., The role of termites and ants in soil modification: a review. *Aust. J. Res*., 1990, **28**, 55–93.
4. Maduakor, H. O., Okere, A. N. and Oneyanuforo, C. C., Termite mounds in relation to the surrounding soil in the forest and derived savanna zones of southeastern Nigeria. *Biol. Fertil. Soil*, 1995, **20**, 157–162.
5. Konate, S., Roux, X. L., Tessier, D. and Lepage, M., Influence of large termitaria on soil characteristics, soil water regime and tree leaf shedding pattern in a West Africa savanna. *Plant Soil*, 1999, **206**, 47–60.
6. Azeredo, G., Morel, J. C. and Barbosa, N. P., Compressive strength of earth mortars. *J. Urban Environ. Eng*., 2007, **1**, 1–4.
7. Abe, S. S., Yamamoto, S. and Wakatsuki, T., Soil-particle selection by the mound-building termite *Macrotermes bellicosus* on a sandy loam soil catena in a Nigerian tropical savanna. *J. Trop. Ecol.*, 2009, **25**, 449–452.
8. Ekundayo, O. E. and Aghatise, O. V., Soil properties of soil mounds under different land use types in a typical Paleudult of Midwestern Nigeria. *Environ. Monit. Assess*., 1997, **45**, 1–7.
9. Lopez-Hernandez, D., Nutrient dynamics (C, N and P) in termite mounds of *Nausutitermes ephratae* from savannas of the Orinoco Lanos (Venezuela). *Soil Biol. Biochem*., 2001, **33**, 747–753.
10. James, R. D. and Loritsch, K. B., Purified quartz and process for purifying quartz. US patent 4983370A, 1991.
11. Venezia, A. M., Parola, V. L., Longo, A. and Martorana, A., Effect of alkali ions on the amorphous to crystalline phase transition of silica. *J. Solid State Chem*., 2001, **161**, 373–378.
12. Alcalá, M. D., Real, C. and Criado, J. M., A new 'incipient-wetness' method for the synthesis of chemically stabilized β-cristobalite. *J. Am. Ceram. Soc*., 1996, **79**, 1681–1684.
13. Perrotta, A. J., Grubbs, D. K., Martin, E. S., Dando, N. R., McKinstry, H. A. and Huarg, C., Chemical stabilization of β-cristobalite. *J. Am. Ceram. Soc*., 1989, **72**, 441–447.
14. Chao, C. H. and Lu, H. Y., β-cristobalite stabilization in (Na_2O + Al_2O_3)-added silica. *Metall. Mater. Trans. A*., 2002, **33**, 2703–2711.
15. Loxley, T. A. and Blackmer, J. F., Cristobalite reinforcement of quartz glass. US patent 5389582, 1995.
16. Awadh, S. M., Geochemistry of termite hills as a tool for geochemical exploration of glass sand in the Iraqi western desert. *Int. J. Geosci*., 2010, **1**, 130–138.
17. Sarcinelli, S. T. *et al.*, Chemical, physical and micromorphological properties of termite mounds and adjacent soils along a toposequence in Zona da Mata, Minas Gerais State, Brazil. *Catena*, 2009, **76**, 107–113.
18. Millogo, Y., Hajjaji, M. and Morel, J. C., Physical properties, microstructure and mineralogy of termite mound materials considered as construction materials. *Appl. Clay Sci*., 2011, **52**, 160–164.

ACKNOWLEDGEMENTS. A.K.G. thanks the Department of Science and Technology, New Delhi for financial support. A.B. thanks the University Grants Commission, New Delhi for a fellowship.

Received 4 May 2013; revised accepted 25 October 2013

Characteristic ULF band magnetic field variations at MPGO, Ghuttu for the 20 June 2011 earthquake in Garhwal Himalaya

Gautam Rawat*

Wadia Institute of Himalayan Geology, 33 GMS Road, Dehradun 248 001, India

Magnetic field variations recorded at the Multi Parameter Geophysical Observatory (MPGO), Ghuttu, using digital fluxgate magnetometer are studied in the frequency band 0.03–1 Hz and for 19–20 h UT for June 2011. Polarization analysis based on planar wave assumption for far field is applied in order to discriminate seismo-magnetic signatures. The dynamics of earthquake processes, considering them as self-organized critical systems, is also studied using fractal dimension of ultra-low frequency band geomagnetic field variations. Marginal increase in polarization ratio and fractal dimension a few days before the earthquake is significant against the background of global geomagnetic activity. At the same time, the effect of post-seismic readjustment of seismogenic processes is clearly marked by significant changes in fractal dimension and increased polarization ratio after the earthquake.

Keywords: Fractals, polarization ratio, seismo-magnetic signatures, ULF band geomagnetic field.

CONSIDERING the hazard earthquakes pose to mankind, it is a natural urge to have algorithms/methodologies which can predict the upcoming earthquakes in a region. However, complexity of the earth system and incomplete understanding of seismogenic processes has hindered this requirement[1]. To achieve this goal or to develop short-term earthquake prediction tools, studies for identification and establishment of earthquake precursory signals

*e-mail: rawatg@wihg.res.in

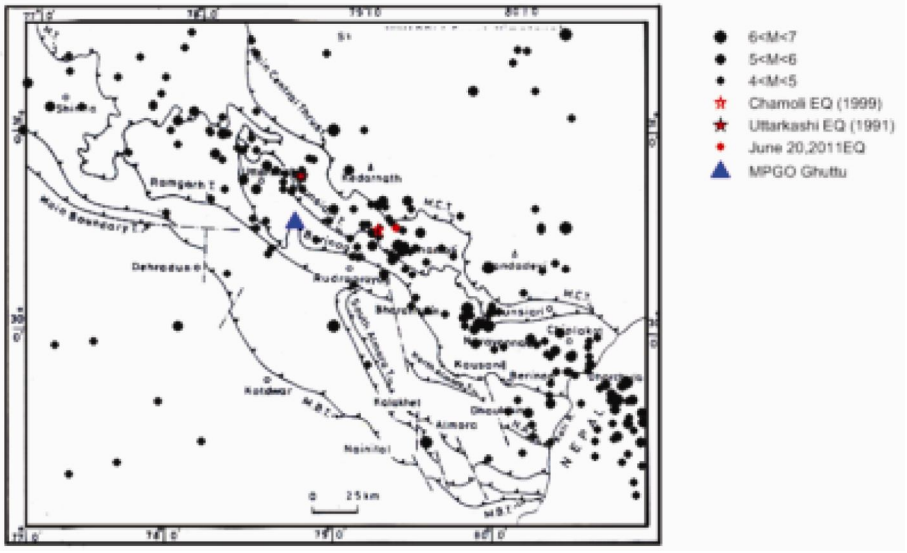

Figure 1. Map showing location of MPGO, Ghuttu, Garhwal Himalaya and distribution of earthquakes with magnitudes greater than 4. Earthquake data are taken from historical catalogue and IMD website.

Table 1. Earthquakes for June 2011 around MPGO, Ghuttu (source: IMD[35]).

Date	Origin time	Epicentre	Depth	Magnitude	Distance from MPGO (km)	Strain radius (km)	Index of seismic activity at Ghuttu[18]
03.06.11	00:53:21	27.5°N, 88.0°E	20	4.9	962	127.9	0.003
15.06.11	00:59:28	30.6°N, 80.0°E	10	3.4	130	28.9	0.014
20.06.11	06:27:18	30.5°N, 79.4°E	12	4.6	63	95.0	0.041
24.06.11	22:13:46	30.0°N, 80.5°E	05	3.2	178	23.77	0.010

in various physical parameters are actively pursued in different countries[2–8]. It is now well established that physical processes in earthquake source region exhibit seismic and magnetic/electromagnetic response. Among the wide variety of precursors, the anomalous electromagnetic (EM) emissions in ultra-low frequency (ULF) band (0.01–10 Hz) have received large attention and are considered as having the potential for short-term earthquake prediction[9–13].

The magnetic field variations observed at the Earth's surface are a composite of contributions from different sources of different scales. Discrimination of weak seismo-magnetic signals from the main field and space-originated magnetic field is therefore a fundamental requirement for identification of any signature of seismo-magnetic origin. Considering weak variations associated with the earthquakes, the seismo-magnetic precursors can be considered as near-field effects[6]. Therefore, polarization ratio[10,13] based on planar wave approximation for fields originated at far-off distances and non-planar waves for near fields, is used to isolate near-field, non-planar seismogenic ULF emissions. Using another approach, fractal dimension variations[14,15], based on self-organized criticality concept can provide information about the dynamics of earthquake preparation processes[10–12,16–18]. In the present study, we present characteristic observations for ULF band magnetic field variations at the Multi Parameter Geophysical Observatory (MPGO), Ghuttu in Northwest Himalaya, for June 2011 obtained after application of these widely used formulations.

We have used digital fluxgate magnetometer (DFM) data recorded at MPGO (30.53°N, 78.75°E; Figure 1). MPGO is a unique state-of-the-art establishment in the Indian subcontinent for earthquake precursory studies in an integrated and organized manner[2]. DFM is being continuously operated with a sampling frequency of 1 Hz. Three-component magnetic field variations of DFM for 19–20 h UT are used to derive polarization ratio and fractal dimension in the frequency band 0.03–0.1 Hz for June 2011. The variations in these two parameters are discussed against the background of earthquake occurrences during that period.

Table 1 gives a list of earthquakes with $M > 3.0$ that occurred within a radius of less than 1000 km from MPGO during June 2011. Two more parameters are shown in the table, namely strain radius[19] and index of seismicity[20]. Strain radius is related with the zone of earthquake preparation. It is believed that effective processes leading to the occurrence of earthquakes are

spatially bounded and this bounded zone is called the earthquake preparation zone. The centre of this zone is considered as the epicentre of the upcoming earthquake. Although there is no definite method for estimating this zone, Dobrovolsky *et al.*[19] gave an empirical relation for calculating strain radius under some physical approximations. Index of seismic activity[20] indicates correlation between seismicity and non-seismic parameters (for example, ULF magnetic field intensity) at the place of observation.

It can be observed that among all earthquakes during June, MPGO is within the preparation zone of an earthquake that occurred on 20 June 2011, according to the Dobrovolsky criterion[19]. Index of seismic activity[20] at MPGO is also higher for this earthquake compared to other earthquakes during the month. It may be further noted that the epicentre of this earthquake is embedded in a narrow belt of concentrated seismicity named as Himalayan Seismic Belt[21]. The area around this also formed the seat of the 1999 Chamoli earthquake (M 6.3) and is currently active as evidenced by the occurrence of seismic swarm[22]. Therefore, it can be expected that some precursory signatures might exist, which can be related to the preparation process of this earthquake.

Ratio of spectral densities of vertical (S_Z) and horizontal magnetic field (S_H) components is called the polarization ratio[11]. The method is based on the assumption that waves (natural EM field) from far-off distances (several thousand kilometres) are planar and therefore do not have vertical component, whereas field of near source origin is non-planar and thus, has vertical component. Thus increased S_Z/S_H ratio indicates presence of near source field. Temporal variations of polarization ratio, in any frequency band, enable us to distinguish seismo-magnetic signals from the background geomagnetic field fluctuations of space origin. We confined our analysis to 1 h data (19–20 UT) for each day centred at local midnight in order to minimize the secondary ionospheric contribution[23]. Figure 2 gives the histogram of daily S_Z/S_H, S_Z/S_y, S_Z/S_x, ratio for the selected hour (19–20 UT) along with K_p variations showing magnetic activity worldwide for entire month of June 2011. The 3 h magnetic index K_p shown corresponds to 18–21 UT (ref. 24) to overlap with time-period whose magnetic data is processed here. S_H is the spectral density of total horizontal component and is calculated as

$$S_H = (S_{x^2} + S_{y^2})^{0.5}.$$

The global geomagnetic variations and polarization ratio are not strongly correlated and the observed S_Z/S_H shows significant variability with mean value of 0.38 ± 0.13. On 3, 5 and 7 June polarization ratio increases above monthly mean, whereas on 15, 16, 18 and 19 June the polarization ratio increased from preceding days up to the month mean. After the earthquake, there are two days (22 and 25 June) when considerably increased polarization ratio is observed.

As the global geomagnetic activity increases, the planar field characterized by nearly vanishing vertical field tends to dominate and hence reduction in polarization ratios below the average value, particularly during prolonged spells of geomagnetic sequences, e.g. 21–25 and 9–14 June 2011, is an expected feature. The isolated large polarization ratios observed on 3, 5 and 7 June before the earthquake and again on 22 and 25 June after the earthquake may manifest complex phase inter-play between planar and non-planar fields. Marginally high ratios starting from 15 June till the occurrence of the earthquake on 20 June, especially when geomagnetic calm prevails, may signify dominance of non-planar source associated with strain build-up close to failure leading to the earthquake.

Bak *et al.*[14] introduced the concept of self-organized criticality and showed that this is the general feature of dynamical systems having spatial degrees of freedom. Critical state of dynamics of such systems can be linked with $1/f$ noise (flicker noise). In this critical state, the system is highly sensitive to any external perturbation whose time response exhibits characteristic of flicker noise (or $1/f$ noise). Earthquake dynamics can be studied based on the self organized criticality (SOC) concept[15], where earthquake occurrence is considered as a critical stage. Earthquake preparation processes, leading to this stage, can be considered the intermediate stage of SOC evolution. Since the dynamics of such a system reflects power law distribution, studying the behaviour of $1/f$ characteristics with time can give information about different

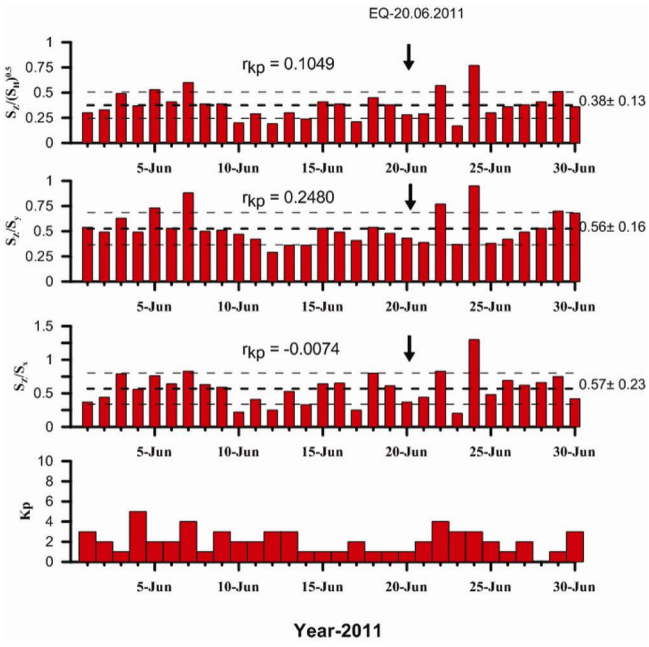

Figure 2. Variability of polarization ratio for June 2013.

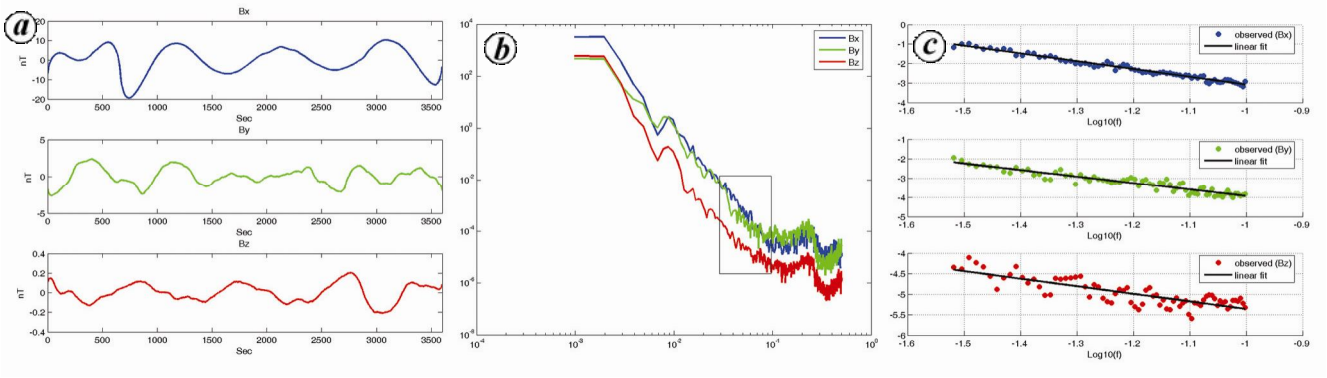

Figure 3. Estimation of spectra slope. ***a***, Time series (19 –20 h) at 1 sec; ***b***, Amplitude spectrum of time series; ***c***, Robust fitting of straight line.

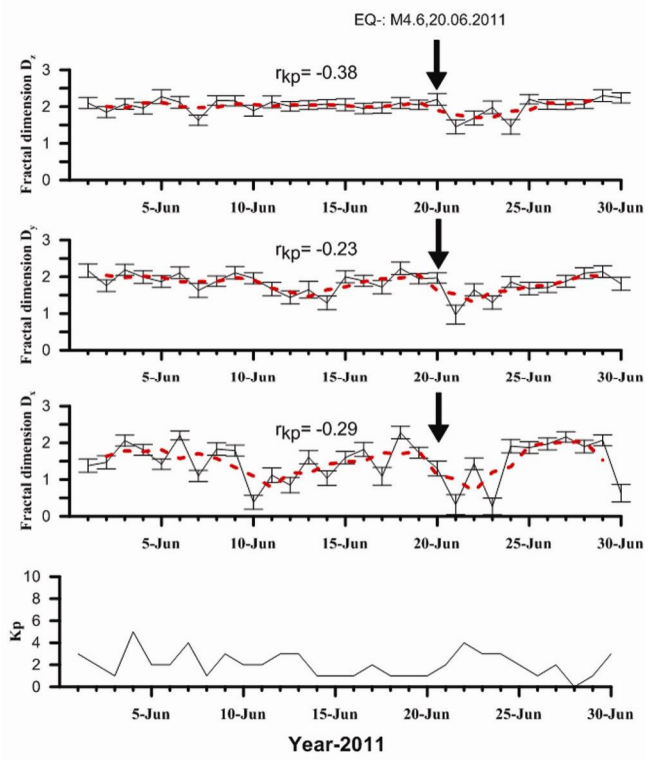

Figure 4. Variability of fractal dimension in the three components of magnetic field for June 2013.

stages of the earthquake preparation process[15–18,25]. In order to study the characteristic $1/f$ behaviour, the slope β of power spectrum behaviour, $s(f) \propto f^{-\beta}$ is obtained from the best-fit line in the log–log plot of selected frequency band. This slope can be linked with fractal dimension using Berry's[26] equation ($D = (5 - \beta)/2$). There are different methods of estimation of fractal dimension[27], e.g. power spectrum (PS), roughness length (RL), semi-variogram (SV), wavelet transform (WT) and re-scaled range (R/S) analysis. Chamoli *et al.*[27] showed that WT and R/S methods are robust and the PS method is not good when data gaps exist. However, in case of continuous datasets, the PS method provides results comparable with other methods (figure 4 of Chamoli *et al.*[27]). We therefore used the PS method to get an initial idea of fractal dimension variability.

To calculate slope of the spectrum, the hourly time series is divided into segments of 1024 data points, with 50% overlapping the previous segment. Each segment is subjected to Fast Fourier Transform. Power spectrum of five segments in 1 h is then averaged to obtain the most coherent and persistent spectral characteristics. Slope (β) of averaged spectrum is then estimated using linear fit to the spectrum plotted on log–log scale (Figure 3) in the frequency band 0.03–0.1 Hz. Seismic activity in NW Himalaya is limited to upper crustal depths and delimited by the geometry of detachment in this part of Himalaya[28]. Recent seismological[29] and magnetotelluric studies[30,31] indicate role of fluids in the earthquakes occurring in this region. Considering the geoelectrical structure of Garhwal Himalaya[30,31], frequency band 0.03–0.1 Hz corresponds to upper crustal and mid-crustal depth. We therefore limited our data analysis for this frequency band, in order to obtain signatures from depths where seismogenic processes dominate in the NW Himalaya.

Fractal dimension (D) is then obtained using Berry's[26] equation utilizing the slope of averaged spectrum. We measure three-orthogonal components of the geomagnetic field variations thus having three sequence of temporal evolution of fractal dimensions corresponding to X (N–S), Y (E–W) and Z (vertical) component respectively (Figure 4). The red dashed line is three days running average of fractal dimension variability.

Fractal dimension variability in three components is found to be different and has negative correlation with K_p variation of 18–21 h UT (Figure 4). The correlation coefficients for fractal dimension variability of each component with K_p variation of 18–21 h for June 2011 are given in Figure 4 above each time series of fractal dimension. Error bars in fractal dimensions are estimated from the errors obtained in the estimation of slope while fitting the straight line to spectra in least square sense.

As intensity of anticipated seismo-magnetic signals in the ULF band is very low, isolation of these signals from the natural background ULF signals of magnetospheric/ionospheric origin is a critical and necessary requirement to investigate the signatures of earthquake precursors. Methods of polarization ratio and fractal dimensions are applied here to the ULF data recorded at MPGO, Ghuttu for June 2011. Control of global geomagnetic activity in the temporal evolution of both polarization ratio and fractal dimension is clearly evidenced respectively, by positive or negative correlation with K_p. However, superimposed on these geomagnetic controlled variations, marginal increase in polarization ratio as well as fractal dimensions is noticed 4–5 days before the earthquake. This increase is significant because geomagnetic activity is low and uniform, for several days before the occurrence of earthquake and may indicate the presence of near-field contribution associated with seismo-magnetic signals. On the basis of strain radius and index of seismic activity for the earthquakes that occurred in June 2011, only the earthquake of 20 June 2011 is expected to produce the seismo-magnetic effect.

An increase in the fractal dimension before earthquakes is reported by different researchers studying seismic electromagnetic phenomena during earthquake preparation processes[16–18,20]. The amplitude of the precursory signal as well as precursory time, i.e. time from the first appearance of the anomaly till the occurrence of the earthquake, vary with the magnitude and distance of the earthquake. Compilation of a variety of precursors also shows that precursory signals tend to increase close to the site of the impending earthquake and precursory time could be shorter for smaller magnitude earthquakes[32]. The increase, both in fractal dimension and polarization ratio 5–6 days before a moderate magnitude (M 4.6) earthquake is in conformity with the emerging scenario. The observation that temporal variability of fractal dimension varies considerably among three components is an important feature. We found fractal dimension variability in X (N–S) magnetic component is more compared to Y (E–W) and vertical component. The fractal dimension for vertical component is more or less stable around the mean value of 2, except for four days (21–24 June 2011), just after the earthquake. The difference in variability in all three components may be linked with the azimuth of primary disturbance. Recent magnetotelluric studies[30,31] have mapped fluid-filled high electrical conductivity ramp structure running parallel to the main central thrust (MCT). The role of high pore-pressure fluids in generating localized seismic activity has been emphasized by seismic tomographic results. Given these evidences of high pore-pressure fluids, electrokinetic effect[33] may be one possible source mechanism for seismo-EM fields for the earthquakes in this region. It also follows that any concentration of stress-induced currents along MCT, in agreement with the observations would produce relatively stronger magnetic effects in X than in Y component. In fact, this direction dependence of propagating seismo-magnetic signals from the source region to multiple measuring sites can be used to locate the source region of seismo-EM signal, i.e. focal zone of impending earthquake[34]. However quantification of such exercise would require long-term monitoring at multiple sites and numerical modelling.

1. Uyeda, S., Nagao, T. and Kamogava, M., Short-term earthquake prediction: current status of seismo-electromagnetics. *Tectonophysics*, 2009, **470**, 205–213; doi:10.1016/j.tecto.2008.07.019.
2. Arora, B. R., Rawat, G., Kumar, N. and Choubey, V. M., Multi-parameter Geophysical Observatory: gateway to integrated earthquake precursory research. *Curr. Sci.*, 2012, **103**, 1286–1299.
3. Yuce, G., Ugurluoglu, D. Y., Adar, N., Yalcin, T., Yaltirak, C., Streil, T. and Oeser, V., Monitoring of earthquake precursors by multi-parameter stations in Eskisehir region (Turkey). *Appl. Geochem.*, 2010, **25**, 572–579.
4. Mauro, D. D., Lepidi, S., Persio, M. D., Meloni, A. and Palangio, P., Update on monitoring magnetic and electromagnetic tectonic signals in Central Italy. *Ann. Geophys.*, 2007, **50**, 51–60.
5. Masci, F., Palangio, P. and Meloni, A., The INGV tectonomagnetic network: 2004–2005 preliminary dataset analysis. *Natl. Hazards Earth Syst. Sci.*, 2006, **6**, 773–777.
6. Gu, Z., Zhan, Z., Gao, J., Yao, T., and Chen, B., Seismomagnetic research in Beijing and its adjacent area, China. *Phys. Chem. Earth*, 2006, **31**, 258–267.
7. Silver, P. G. and Wakita, H., A search for earthquake precursors. *Science*, 1996, **273**, 77–78.
8. Bakun, W. H. and Lindh, A. G., The Parkfield, CA earthquake prediction experiment. *Science*, 1985, **229**, 619–624.
9. Molchanov, O. A. and Hayakawa, M., Seismo-electromagnetics and related phenomena: History and results. Terrapub, Tokyo, 2008, p. 189.
10. Hayakawa, M., Hattori, K. and Ohta, K., Monitoring of ULF (ultra-low-frequency) geomagnetic variations associated with earthquakes. *Sensors*, 2007, **7**, 1108–1122.
11. Hayakawa, M., Kawate, R., Molchanov, O. A. and Yumoto, K., Results of ultra-low-frequency magnetic field measurements during the Guam earthquake of 8 August 1993. *Geophys. Res. Lett.*, 1996, **23**, 241–244.
12. Park, S. K., Johnston, M. J. S., Madden, T. R., Morgan, F. D. and Morrison, H. F., Electromagnetic precursors to earthquakes in the ULF band – a review of observations and mechanisms. *Rev. Geophys.*, 1993, **31**, 117–132.
13. Hirano, T. and Hattori, K., ULF geomagnetic changes possibly associated with the 2008 Iwate–Miyagi Nairiku earthquake. *J. Asian Earth Sci.*, 2011, **41**, 442–449.
14. Bak, P., Tang, C. and Wiesenfeld, K., Self-organized criticality: an explanation of 1/*f* noise. *Phys. Rev. Lett.*, 1987, **59**, 381–384.
15. Dimri, V. P. (ed.), Fractals in geophysics and seismology: an introduction. In *Fractal Behaviour of the Earth System*, Springer, New York, 2005, p. 207.
16. Hayakawa, M., Itoh, T. and Smirnova, N., Fractal analysis of ULF geomagnetic data associated with the Guam earthquake on 8 August 1993. *Geophys. Res. Lett.*, 1999, **26**, 2797–2800.
17. Ida, Y. and Hayakawa, M., Fractal analysis for the ULF data during the 1993 Guam earthquake to study prefracture criticality. *Nonlinear Process. Geophys.*, 2006, **13**, 409–412.
18. Gotoh, K., Hayakawa, M., Smirnova, N. A. and Hattori, K., Fractal analysis of Seismogenic ULF emissions. *Phys. Chem. Earth*, 2004, **29**, 419–424.

19. Dobrovolsky, I. P., Zubkov, S. I. and Myachkin, V. I., Estimation of the size of earthquake preparation zones. *Pageoph*, 1979, **117**, 1025–1044.
20. Molchanov, O., Schekotov, A., Fedorov, E., Belyaev, G. and Gordeev. E., Preseismic ULF electromagnetic effect from observation at Kamchatka. *NHESS*, 2003, **3**, 203–209.
21. Arora, B. R., Gahalaut, V. K. and Kumar, N., Structural control on along-strike variation in the seismicity of the northwest Himalaya. *J. Asian Earth Sci*., 2012, **57**, 15–24; doi: 10.1016/j.jseaes.2012.06.001.
22. Paul, A. and Sharma, M. L., Recent earthquake swarms in Garhwal Himalaya: a precursor to moderate to great earthquakes in the region. *J. Asian Earth Sci*., 2011, **42**, 1179–1186.
23. Trivedi, N. B., Arora, B. R., Padilha, A. L., Da Costa, J. M. and Dutra, S. L. G., Global Pc5 geomagnetic pulsations of March 24, 1991, as observed along the American sector. *Geophys. Res. Lett*., 1997, **24**, 1683–1686.
24. ftp://ftp.ngdc.noaa.gov/STP/GEOMAGNETIC_DATA/INDICES/KP_AP
25. Smirnova, N., Hayakawa, M. and Gotoh, K., Precursory behaviour of fractal characteristics of the ULF electromagnetic field in seismic active zones before strong earthquakes. *Phys. Chem. Earth*, 2004, **29**, 445–451.
26. Berry, M. V., Diffractals. *J. Phys. A: Math. Gen.*, 1979, **12**, 207–220.
27. Chamoli, A., Bansal, A. R. and Dimri, V. P., Wavelet and rescaled range approach for the Hurst exponent for short and long irregular time series. *Comput. Geosci.*, 2007, **33**, 83–93.
28. Kayal, J. R., Ram, S., Singh, O. P. and Karunakar, G., Aftershocks of the March 1999 Chamoli earthquake and seismotectonic structure of the Garhwal Himalaya. *Bull. Seismol. Soc. Am.*, 2003, **93**, 109–117; doi: 10.17851/0119990139.
29. Mahesh, P., Gupta, S., Rai, S. and Sharma, P. R., Fluid driven earthquakes in the Chamoli region, Garhwal Himalaya: evidence from local earthquake tomography. *Geophys. J. Int*., 2012, **191**, 1295–1304.
30. Israil, M., Tyagi, D., Gupta, P. K. and Sri Niwas, Investigations for imaging electrical structure of Garhwal Himalaya corridor, Uttarakhand, India. *J. Earth Syst. Sci.*, 2008, **117**, 189–200.
31. Rawat, G., Electrical conductivity imaging of Uttaranchal Himalaya using MT method. Ph D thesis, Department of Earth Sciences, IIT Roorkee, Roorkee, 2012.
32. Cicerone, R. D., Ebel, J. E. and Britton, J., A systematic compilation of earthquake precursors. *Tectonophysics*, 2009, **476**, 371–396; doi: 10.1016/j.tecto.2009.06.008.
33. Mizutani, H., Ishido, T., Yokokura, T. and Ohnishi, S., Electrokinetic phenomena associated with earthquakes. *Geophys. Res. Lett*., 1976, **13**, 365–368.
34. Dudkin, F., Rawat, G., Arora, B. R., Korepanov, V., Leontyeva, O. and Sharma, A. K., Application of polarization ellipse technique for analysis of ULF magnetic fields from two distant stations in Koyna–Warna seismoactive region, West India. *NHESS*, 2010, **10**, 1–10; doi:10.5194/nhess-10-1-2010.
35. http://www.imd.gov.in/section/seismo/dynamic/last-monthJun11.htm

ACKNOWLEDGEMENTS. I thank the Director, Wadia Institute of Himalayan Geology, Dehradun for the necessary support to carry out the work. Financial support from MoES to the MPGO-EPR project through MoES/P.O.(Seismo)/NPEP(15)/2009 is acknowledged. I also thank Dr B. R. Arora (former Director, WIHG) for guidance and motivation and the anonymous reviewers for their critical reviews and suggestions.

Received 3 August 2013; revised accepted 11 November 2013

Large capacity reaction floor-wall assembly for pseudo-dynamic testing at IIT Kanpur and its load rating

Durgesh C. Rai[1,*], Sudhir K. Jain[2], C. V. R. Murty[3] and Dipanshu Bansal[4]

[1]Department of Civil Engineering, Indian Institute of Technology Kanpur, Kanpur 208 016, India
[2]Indian Institute of Technology Gandhinagar, Ahmedabad 382 424, India
[3]Indian Institute of Technology Jodhpur, Jodhpur 342 011, India
[4]Department of Civil Engineering, State University of New York at Buffalo, USA

The earthquake simulation on full-scale civil engineering structures in a pseudo-dynamic testing facility provides an affordable and practical means to understand the seismic behaviour of structures as it provides accurate information about their real time response of inelastic behaviour up to failure. One such pseudo dynamic testing facility is nearing completion at IIT Kanpur, which has 15 m × 10 m L-shaped and 10.5 m high reaction wall and 1.2 m thick top slab of the box girder for the strong floor. The anchor points are located in the wall and floor in a square grid of 0.6 m with each point has load capacity of 1.7 MN in tension and 1.0 MN in shear. The 2 m thick post-tensioned wall using Freyssinet 12K15 cable system in a novel configuration can resist an overturning moment of 12.7 MNm per metre of the wall. The capacity of the reaction assembly depends upon number of loads applied, combination of loads and interaction between different components of the reaction assembly structure. A methodology based on 'influence coefficients' was developed to estimate the worst load combination for describing load rating of the reaction structure. Finite element analyses in ABAQUS environment were conducted to compute the influence coefficients matrix whose elements can be added linearly to find out the maximum loading effect on the reaction structure which can be used to determine the limiting load for a particular case of load application.

Keywords: Pseudo-dynamic testing facility, reaction wall, seismic behaviour, load rating.

THE survival of conventional structures during earthquakes depends on their ability to deform inelastically and dissipate seismic energy. The performance evaluation of their energy dissipation potential is difficult by analytical methods due to their complex inelastic behaviour. As a result, experimental testing is most commonly employed to study the inelastic behaviour of structures in earthquake-type loads. The pseudo-dynamic test (PDT) is an experimental technique for simulating the earthquake response of structures and structural components in time

*For correspondence. (e-mail: dcrai@iitk.ac.in)